10ème Congrès Français d'Acoustique
*Lyon, 12-16 Avril 2010*

# Ultrasonic Far-Field Holography of Point Scatterers and Interfaces

Sergey A. Tsysar[1], Oleg A. Sapozhnikov[1,2]

[1]Department of Acoustics, Physics Faculty, Moscow State University, Leninskie Gory, Moscow 119991, Russia, sergey@acs366.phys.msu.ru
[2]Center for Industrial and Medical Ultrasound, Applied Physics Laboratory, University of Washington, Seattle, WA, USA, oleg@acs366.phys.msu.ru

Modern ultrasound imaging is usually performed using pulse-echo principle, i.e. it utilizes backscattering of short acoustic pulses. In contrary, conventional optical imaging is based on continuous light waves. Similar approach is possible in acoustics as well. Holography is a method of recording wave scattering from an object such that the object's shape and position can be reconstructed later. The holographic approach used here relies on the principle of a time-reversal mirror and the Rayleigh integral. An ultrasonic beam consisting of long tone bursts is directed at a target object and the resulting acoustic field is measured at a large number of points surrounding the object. A computer-controlled positioning system is used to scan a small broadband hydrophone across a grid of measurement points in a single surface near the target. Object reconstruction is then accomplished numerically by back-propagating of the acoustic field from measurement locations to a 3D region representing the object. Theoretically, the accuracy and the optimal parameters of the method were studied by modeling forward and backward propagation from a point scatterer. Experimentally set of 3-mm diameter plastic beads and a piece of styrofoam with a rough surface and a diameter of several cm were investigated. Ultrasound frequencies from 1 to 4 MHz were considered, while hologram measurements were collected with grid spacings between 0.2 and 0.4 mm. Using this 3D ultrasonic holography method, it is possible to reconstruct the position and shape of objects or collections of objects that do not involve a significant amount of multiple scattering. Because the spatial resolution of the method has a typical diffraction limit on the order of a wavelength, improved spatial resolution can be achieved with higher frequencies and increased angular size of scanning region.

## 1 Introduction

3D ultrasound imaging is usually performed using backscattering of short acoustic pulses [1, 2]. In contrary, conventional optical imaging is based on continuous light waves. Similar approach is possible in acoustics as well. Hologram recorded using continuous waves (c.w.) in some cases can be a useful alternative to the pulse-echo technique. For instance, near-field acoustical holography makes it possible to resolve details smaller than wavelength [3, 4]. In this paper we demonstrate a possibility of acoustical holography in 3D based on 2D hydrophone scans with a use of monochromatic c.w. ultrasound.

Holography is a method of recording wave scattering from an object such that the object's shape and position can be reconstructed later. In our previous work, we demonstrated experimentally that 2D recording of the wave amplitude and phase by means of a single hydrophone scanning can be used to reconstruct surface vibration pattern of megahertz frequency range piezoelectric transducers [5]. The method consists of several steps. First, the amplitude and the phase of acoustic pressure are measured along a certain plane in front of the transducer. Then the phase sign is changed, i.e. the wave is phase-conjugated, and the vibration velocity, pressure or displacement of the source surface is numerically calculated using Rayleigh integral. Employing such an approach, many transducers of different size and shape, both plane and focused, with working frequencies from 0.5 to 3 MHz, including piezocomposite transducers and transducers with damaged surfaces were studied [6]. It was shown that the method possesses high precision and a spatial resolution about a wavelength, and it can be successfully applied in liquids for quantitative investigation of surface vibration pattern of different transducers, which in turn allowed to predict very fine details of the radiated ultrasonic fields. Moreover, method can be extended to the transient regime [7].

In addition to such measurements of surface vibration, it is of practical interest to record acoustical holograms of 3D objects.

## 2 Theoretical aspects of far-field holography of 3D objects

### 2.1 Point scatterers

In the present work, we use acoustical holographic reconstruction in the form similar that used in optics, i.e. not only for obtaining of acoustic field distribution on a transducer surface, but for obtaining information on an object that has three-dimensional nature. Consider a set of several small (as compared to wavelength) scatterers, which are exposed to ultrasonic beam generated by a transducer (Fig. 1a). Information about amplitude and phase of acoustic field is collected on a reference surface *S*. Here we use forward scattering and measure the “shadow” field. In order to find the part of the field that comes only from the scatterers, i.e. scattered field, in case of such geometry it is necessary to subtract acoustic field that is radiated by the transducer in the absence of the scatterers, i.e. free field, from the field that appears when the scatterers are present. Using the Rayleigh integral and time-reversal principle [8] we calculate back-propagation of the scattered field, and

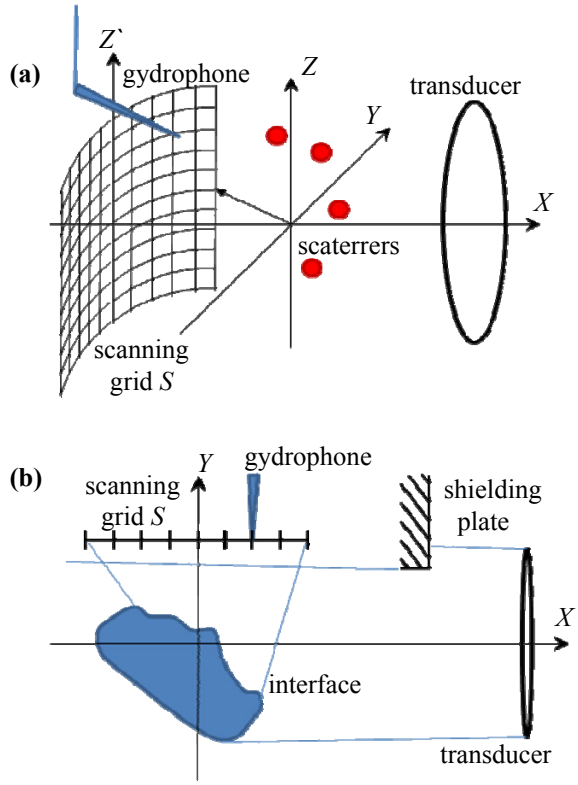


Figure 1. Setup for acoustical holography experiments (a) for point scatterers; (b) for interfaces (top view).

from this pressure pattern find the 3D position of the scatterers.

Experimentally, it is easier to perform hydrophone scanning along a plane reference surface. We first used this approach for recording a hologram, i.e. for collecting amplitude and phase of scattered field. The Rayleigh integral over the scanning surface $S$ ($z \equiv 0$) was used to perform numerical backward propagation of the field:

$$p_{sc}(x,y,z) = 2\int_S p_{sc}(x',y',0)\frac{\partial G^*}{\partial n}dx'dy', \qquad (1)$$

where $p_{sc}(x, y, z)$ is acoustic pressure complex amplitude of the scattered field; $x$, $y$, and $z$ are spatial coordinates; $x'$,$y'$ are coordinate of the surface element $dx'dy'$ on the surface $S$. The operator $\partial/\partial n$ denotes derivative in the direction perpendicular to the surface $S$, symbol * means phase conjugation, and $G$ is the free space Green's function

$$G = \frac{e^{ikR}}{4\pi R}. \qquad (2)$$

Here $R = \sqrt{(x-x')^2 + (y-y')^2 + z^2}$ and $k = \omega/c$ is wavenumber. In case of plane reference surface we have

$$\frac{\partial G^*}{\partial n} = \frac{\partial G^*}{\partial z} = -\frac{1}{4\pi}\frac{z}{R^3}(ikR+1)e^{-ikR}. \qquad (3)$$

Using (1)-(3), one can obtain expression for 3D pressure distribution of the scattered field amplitude:

$$p_{sc}(x,y,z) = -\frac{1}{2\pi}\int_S p_{sc}(x',y',0)\frac{z}{R^3}(ikR+1)e^{-ikR}dx'dy'. \qquad (4)$$

Although the left-hand side function is marked here as "scattered field", the result of integration based on (4) differs from the true scattered field. This happens because the Green's function (3) does not account for disappearance of a time-reversed convergent spherical waves when they come to the origin of the primary waves (i.e. diverging spherical waves) [8]. In practice this results in smearing out the reconstructed images of point scatterers.

Theoretically, the accuracy and the optimal parameters of the holography method were studied by modeling forward and backward propagation from a point scatterer. The calculations show that the image of a point scatterer has a shape of an ellipsoid with lateral size on the order of a wavelength and a somewhat larger axial size (i.e. in the direction perpendicular to the scanning plane).

Axial resolution can be improved by increasing angular size of scanning surface. This can be done either by increasing size of the plane scanning surface, or by using instead curved surface that surrounds the studied object. For a positioning system with a rotational degree of freedom (in addition to translations), it is convenient to use cylindrical scanning surface. For a reference surface $S$ having shape of a cylinder of radius $R_0$, the integral (1) can be written as

$$p_{sc}(x,y,z) = -\frac{1}{2\pi}\int_S p_{sc}(R_0\cos\varphi, R_0\sin\varphi, z')\frac{\beta}{R^3}(ikR+1)e^{-ikR}dS, \qquad (5)$$

where

$$\beta = (R_0\cos\varphi - x)\cos\varphi + (R_0\sin\varphi - y)\sin\varphi, \qquad (6)$$

$$R = \sqrt{(R_0\cos\varphi - x)^2 + (R_0\sin\varphi - y)^2 + (z'-z)^2}. \qquad (7)$$

Here, $\varphi$ and $z'$ are cylindrical coordinates of the surface element $dS$.

### 2.2 Interfaces

Contrary to point scatterers, insonification of a large object results in a stronger scattered field that can be detected reliably even when the hydrophone is placed outside the original incident beam. In doing so, one can avoid the procedure of subtracting of the incident acoustic field. The possible experiment geometry is shown in Fig.1b. Here, a shielding plate is used to prevent direct exposure of the measurement surface $S$ by the transducer beam.

For a plane reference surface the Rayleigh integral (1) over the scanning surface $S$ was used to perform numerical backward propagation of the field.

A known drawback of using a monochromatic wave is speckle pattern that appears when the scattering object surface has dimensions larger than a wavelengh. In order to reduce this artifact when reconstructing the object shape, we employed a special smoothing algorithm. To achieve appropriate resolution, we used relatively high frequency (4 MHz).

## 3 Experimental arrangement and results of measurements

### 3.1 Point scatterers

Measurements were performed with 3-mm diameter plastic beads placed in a water tank (Fig. 3a). A piezoelectric transducer (flat or concave) was placed in the water tank and directed towards a target objects. The source was excited by a long tone burst to simulate c.w. regime. The frequency was chosen in the range from 1 to 1.5 MHz. The acoustic wave propagated in water towards the objects and scattered at them. The resulted acoustic field was measured by a small receiver placed at some distance from the object. Thanks to possibility of repetitive excitation of the source, a single receiver allowed to perform pressure measurements in a big number of spatial points. To do so,

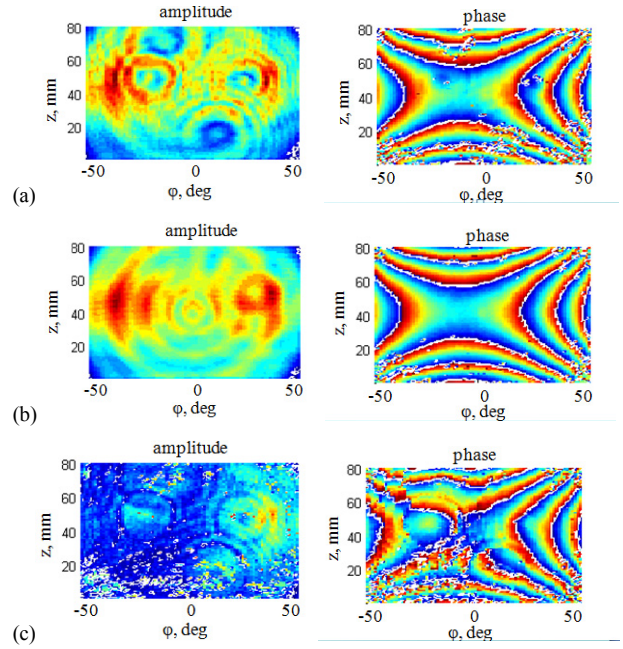


Figure 2. Amplitude and phase distribution measured along a cylindrical surface with $R_0$ = 45 mm. Working frequency is 1 MHz. Acoustic field parameters are shown, from top to bottom, for the following cases: (a) in the presence of scatterers; (b) in the absence of scatterers; (c) after subtraction and phase conjugation (see the text for details)

the hydrophone was scanned, i.e. moved point-after-point along a reference surface. This scanning surface was located behind the scatterers, relative to the transducer. Phase and amplitude measurements were performed by a small broadband hydrophone (SEA, PVDFZ44-0400, sensitivity region size 0.4 mm). The hydrophone was moved along scanning surface with a fixed step using a computer-controlled positioning system (Velmex-UnislideVP9000). Measurements were collected with a grid spacing between 0.3 and 0.4 mm depending on distance between surface and 3D object. Fig. 2a shows example of the amplitude and phase distributions measured along a cylindrical surface with the curvature radius $R_0$ = 45 mm for 1 MHz reference tone signal.

The experiment was divided in three steps.

First, acoustic parameters were collected in the presence of scatterers (Fig. 1a).

On the second step the scatterers were removed from the tank and acoustic field radiated by the transducer was measured on the same surface that was used during the first step. Figure 2b shows example of amplitude and phase distribution along the cylindrical surface for 1 MHz reference tone signal in the absence of the scatterers.

On the third step object reconstruction was accomplished numerically by field subtraction described in previous section. Back-propagation is calculated for the acoustic field using Eqs. (4) or (5) for plane and cylindrical surfaces, respectively. This gives a 3D representation of the object. Field parameters on cylindrical surface after performing procedures of subtraction and phase conjugation are plotted in Fig. 2c.

The isosurfaces with 0.8 level from maximum amplitude value, calculated from the plane surface, are presented in Fig. 3b. High-amplitude regions represent images of scatterers. It is seen that those regions is fairly distinct, and their centers coinside with position of the real scatterers.

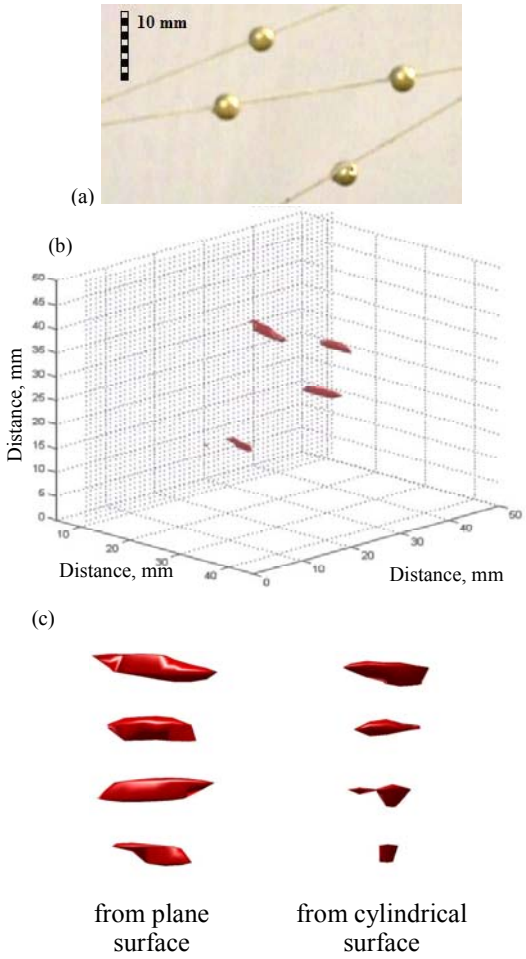


Figure 3. (a) Set of 3-mm diameter plastic beads; (b) isosurfaces with 0.8 level from maximum amplitude value calculated from the plane surface; (c) shape of the isosurfaces with 0.8 level from maximum amplitude value calculated from the plane (left) and cylindrical (right) surfaces.

Scatterer image size in lateral direction (relative to the scanning plane) is about 3 mm. In axial direction it varies from 5 to 7 mm for different scatterers. In case of the cylindrical scanning surface position of the images also agrees well with the position of the real scatterers (Fig. 3c). Reconstructed image size in lateral direction is about 3 mm, and in axial direction it varies from 3 to 5 mm. Thus, use of the cylindrical surface allows to improve axial resolution with the same numbers of scanning points.

### 3.2 Interfaces

Measurements were performed with a piece of Styrofoam having rough surface and a diameter of 4 cm (Fig.4a). The studied part of the object surface was specially shaped and had three specific features: an indentation in the shape of a convex hemisphere, a height in the shape of a concave hemisphere, and a groove in the shape of a convex elongated strip. The chosen working frequency was 4 MHz. The measurement procedure was similar to the previous one, but in this case we measure whole scattered field along reference surface $S$ at once. Therefore, number of experimental steps is reduced from 3 to 2. On the first step scattered field measurements were performed. On the second step object reconstruction was

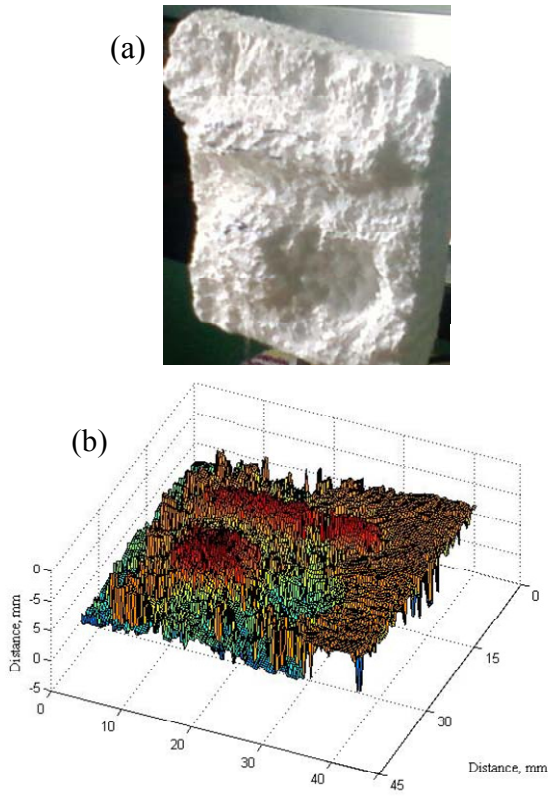


Figure 4. (a) Surface of Styrofoam sample.
(b) Reconstructed surface of Styrofoam sample.

accomplished numerically by procedure described in section 2.2. Reconstructed surface is represented in Fig. 4b.

# 4 Conclusion

Using the proposed 3D ultrasonic holography method, it is possible to reconstruct position and shape of scattering objects in the cases when multiple scattering is not essential. Because the spatial resolution of the method has a typical diffraction limit on the order of a wavelength, improved spatial resolution can be achieved with higher frequencies.

# Acknowledgment

Work supported by RFBR 08-02-00368, ISTC 3691 and NIH R01EB007643.

# References

[1] G. S. Kino, Acoustic Waves: Devices, Imaging, and Analog Signal Processing, *Prentice-Hall, Englewood Cliffs, N.J.*, 1987.

[2] F. W. Kremkau. Diagnostic Ultrasound: Principles and Instruments, *7th ed. Philadelphia: Elsevier/Saunders*, 2006.

[3] E. G. Williams, Fourier Acoustics: Sound Radiation and NAH, *London: Academic*, 1999.

[4] E. G. Williams and J. D. Maynard, "Holographic imaging without the wavelength resolution limit," *Phys.Rev.Lett.*, vol. 45, pp. 554–557 (1980).

[5] O.A. Sapozhnikov, Yu.A. Pishchalnikov, and A.V. Morozov, "Reconstruction of the normal velocity distribution on the surface of an ultrasonic transducer from the acoustic pressure measured on a reference surface," *Acoustical Physics*, vol. 49, no. 3, pp. 354–360 (2003).

[6] O. A. Sapozhnikov, A. V. Morozov, and D. Cathignol, "Piezoelectric transducer surface vibration characterization using acoustic holography and laser vibrometry," *Proceedings of 2004 IEEE UFFC 50th Anniversary Joint Conference* (Montreal, Canada, August 23-27, 2004), pp.161-164 (2004).

[7] O. A. Sapozhnikov, A. E. Ponomarev, and M. A. Smagin, "Transient acoustic holography for reconstructing the particle velocity of the surface of an acoustic transducer," *Acoustical Physics*, vol. 52, no. 3, pp. 324–330 (2006).

[8] M. Fink, "Time Reversed Acoustics," pp. 34-40, *Physics Today*, March 1997.